INTERNATIONAL JOURNAL OF APPLIED SCIENCE AND ENGINEERING REVIEW

ISSN: 2582-6271

Vol.1 No.2; 2020

THE EFFECT OF TEMPERING TEMPERATURE ON THE CORROSION SUSCEPTIBILITY OF 0.42%C STEEL IN SODIUM CHLORIDE (NACL) ENVIRONMENT

Obogai L.E[1], Obidimma D. Ikeh[2] and Anioke S.A[3].

[1]Department of Mechanical Engineering, Federal University Utuoke, P.M.B 126, Yenagoa.

[2]Department of Mechanical Engineering, University of Benin P.M.B 1154, Benin City.

[3]Department of Metallurgical and Materials Engineering, Enugu State University of Science and Technology.

ABSTRACT

This paper presents the results of an investigation on the effects of tempering temperatures on the corrosion susceptibility of 0.42%C (medium carbon). Heat treatments were carried out on prepared samples in stages. The first was austenitizing the samples followed by quenching and then tempering at 250˚C, 350˚C, 450˚C, 550˚C with holding time of 30minutes and with un-heat treated one. All specimens were prepared for electrochemical test in NaCl solution and metallographic study of the samples was also done. The open circuit potential (OCP), corrosion test and polarization resistance measurement were carried out to determine the rate of corrosion. The 550˚C tempered sample has lower corrosion rate of 0.5 mm/yr than samples tempered at 450˚C, 350˚C and 250˚C, which demonstrated that, the corrosion resistance of tempered 550˚C sample is higher than other samples. The result also showed a decrease in corrosion current ICorr (-20.582 to -3.722) μA during the potential sweep from the least tempered specimen to the highest, micrographic images also revealed presence of cementite precipitate in the tempered martensite which became coarse as the tempering temperature increased.

KEYWORDS: Heat Treatment, Microstructure, Cementite, Ferrite, Pearlite

INTRODUCTION

There is a great wealth of metallurgical evidence demonstrating the relevance of studying the corrosion of engineering materials, including various ways of improving their corrosion resistance among others. Research has highlighted the risk of failures due to corrosion particularly in pipelines among other industrial facilities [1]. Even though the freely corroding carbon steel materials used in the past have been replaced with modern corrosion resistant super alloys, material selection factors such as cost, availability and performance remain the reason why carbon steels are still been used. Some risk implications of corrosion in oil and gas facilities includes economic loss, destruction of the ecosystem, pollution of the environment, and the likelihood of explosion/fire outbreak depending on the instantaneous release of the product [2]. Therefore, it is not a surprise that the research on the corrosion and corrosion protection of metallic materials is developed on a large scale in different directions and a wide range of engineering decisions. For all that, the improvement of corrosion behaviour of metals and alloys still stays as one of

ISSN: 2582-6271

Vol.1 No.2; 2020

the most important engineering problems in the area of material selection applications [3]. Steel is an alloy of iron with definite percentage of carbon ranging from 0.002-2.0%. The presence of carbon in iron gives steels its remarkable properties. Steels with carbon content varying from 0.25% to 0.5% is classified as medium carbon steel [4]. Medium carbon steel is relatively cheap and commercially available in Nigeria when compared to alloy steels. Due to its amenability to heat treatment processes and wide range of mechanical properties which can be enhanced (ranging from strength to toughness), medium carbon steel is widely used in the production of structural steels, machine parts such as bolts, gears, wire rods, and railway tracks. Unfortunately, corrosion has proved to be a major threat to its favourable mechanical properties. According to Ferhat et al. [5], corrosion rate in carbon steels depends on the carbon composition as well as the structure formed due to prior heat treatment and increases with carbon content. The extent of the increase depends largely on prior heat treatment; on slowly cooling carbon steel from the austenite phase, cementite in part assumes a lamellar shape, forming pearlite [6]. This structure corrodes at a comparatively low rate because of the relatively massive form of cementite formed by decomposition of austenite compared with smaller-size cementite particles resulting from decomposition of martensite. Pearlitic structures corrode faster than spheroidized ones, and steels containing fine pearlite corrode more rapidly than those with coarse pearlite [7]. The importance of the amount of cementite acting as cathode and its state of subdivision both supports the electrochemical mechanism of corrosion. During tempering as Post Weld Heat Treatment (PWHT) process, weldments are subjected to grain refinement, and this process alters grain size, boundary and density in carbon steels [8]. Ultimately, these changes may have an impact on the electrochemical behaviour and, consequently, corrosion susceptibility, hence the need to investigate experimentally the corrosion susceptibility of tempered 0.42%C steel in NaCl environment [9].

MATERIALS AND METHOD

3.1 Samples Preparation

The specimen, received in ribbed form, was machined to 12mm gauge diameter so as to remove the ribs. Ten samples of 20mm length were then cut with the aid of hacksaw respectively. The simulated corrosion medium was prepared by dissolving 58.44g of NaCl in 1 litre distilled water to make up 1 Molarity solution. The solution was stirred to have a uniform concentrated. Preparation of the specimen for corrosion test was done by soldering an insulated copper wire to the base of the specimens using a lead based solder. Insulation of the specimen was carried out with a cast of polyester resin mixed with hardener and accelerator reagent. A surface area was exposed for the test which was abraded to smooth finish using emery papers. The specimens were then cleaned in ethanol before being immersed in the electrolyte for corrosion testing.

3.2 Heat Treatment

ISSN: 2582-6271

Vol.1 No.2; 2020

The heat treatment process was carried out with a muffle furnace. The furnace was preheated to the austenite temperature (850oC) before the specimens were placed. Eight specimens were heated at 850oC – a temperature in the region of 30 – 50oC above the A1 (upper critical temperature) line of the Fe – Fe3C phase diagram. At 850oC the specimens were held for 45 minutes to ensure uniform homogeneity. In order to enhance the hardness, the red hot samples were rapidly cooled in water. A pair of specimen was tempered at 250oC, 350oC, 450oC, 550oC so as to guarantee the reliability of the process. The specimens were held at these temperatures for 30minutes and were allowed to air cool to ambient temperature after tempering. Two other specimens were also set aside to serve as control for the assessment of the heat treated ones.

3.3. Corrosion Test

The potentiostat was programmed to perform a scan by accepting a computer generated waveform with a pre-set scanning range of ±250mV about ECorr (open circuit potential). Beginning the scan from -250mV vs. ECorr a continuous scan was carried out up to +250mV vs. ECorr with a scan rate of 1mV/sec. The anodic and cathodic plots were both plotted on a graph. From the data generated from the scan, the potential versus the logarithm of the current was plotted using VersaStudio software. To obtain the corrosion current and polarization resistance, a region about ECorr was selected and the software automatically extrapolated the linear portion of the curves to determine the point of intercept. The point of interception is the corresponding ICorr value. By clicking on the tafel slope analysis tool the Tafel anodic constant (βA) and Tafel cathodic constant (βC) were calculated automatically from the linear portion of the curves. The corrosion rate estimate was obtained from the corrosion current ICORR, the slopes of the curves obtained from the intercept of the two linear segments RP. The following formula shows the relationship between the Rp (polarization resistance) and corrosion current ICorr.

The corrosion current, ICorr, is obtained from the Tafel plot by extrapolating the linear portion of the curve to ECorr.
Corrosion rate (CR) = Corrosion Rate (mpy) = 0.13 (I_Corr (E.W))/d.
E.W. = equivalent weight of the corroding species,
d = density of the corroding species, g/cm2.

3.4 Microstructural Examination

The specimens were hot mounted (at around 200°C) in a mounting press using a thermosetting plastic to allow for easy handled during surface preparation. Mounted specimens were grounded with rotating discs of abrasive paper flushed with a suitable coolant to remove debris and heat. The grade coarseness of the emery papers used progressively is 180, 220,320,400,600,800 and 1200 grit size. Between each grade the specimen was washed thoroughly with soapy water to prevent contamination from coarser grit present on the specimen surface. Polishing discs covered with soft cloth impregnated with colloidal silica suspension

ISSN: 2582-6271

Vol.1 No.2; 2020

Specimen	E_{CORR} mV/SSE	β_C mV/dec	β_A mV/dec	I_{CORR} (μA)	R_P Ω/cm^2	CR (mmpy)
Control	-581.093	306.286	67.262	-78.359	-0.30601	0.90926
250°C Tempered	-619.924	145.801	91.81	-20.582	-1.19006	0.23883
350°C Tempered	-630.78	97.859	67.582	-12.211	-1.42334	0.14170
450°C Tempered	-612.846	182.849	57.759	-6.842	-2.78927	0.07940
550°C Tempered	-632.124	112.339	33.14	-3.722	-2.98936	0.04319

solution was used for the final stage. Colloidal particles of two different grades were used: a coarser polish - typically with silica particles 6 microns in diameter and a finer polish – typically with silica particles. An etching solution containing 2% Nitric acids and 98% methylated spirit was applied on the polished surfaces for 2 minutes before rinsing with water. Microstructure examination of the etched surface of all the specimens was carried out using an optical microscope. The micrograph images were taken at a magnification X400. Figures 4.8- 4.12 represent micrographs of the structures obtained from the specimens and the changes which ensued as the specimens were tempered.

4.1 Results

Table 4.1. Electrochemical Parameters deduced from Tafel Plot

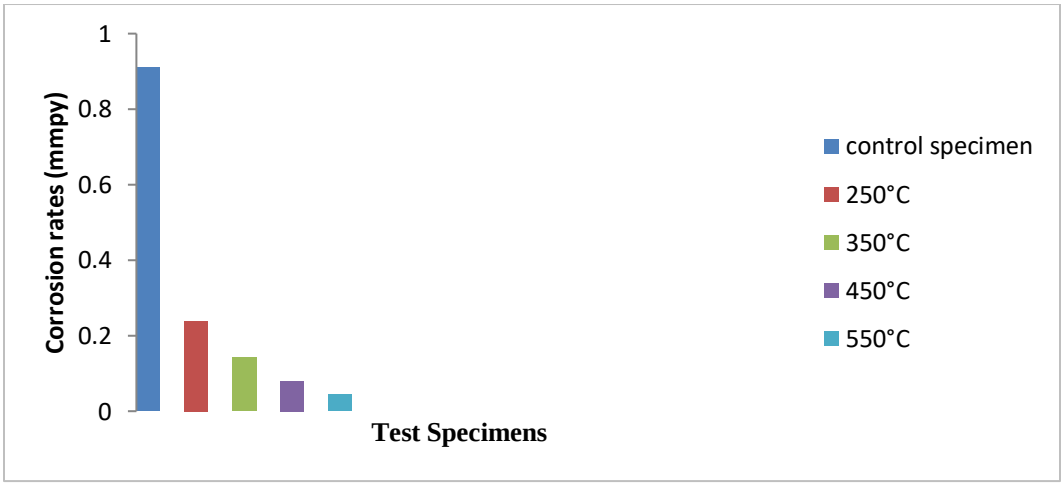

Figure 4.1. Chart Comparing the Corrosion Rate of the Specimens

Presents the corrosion rate of the tempered and control specimens. The chart shows a significant drop in the corrosion rate of the tempered specimens compared to the control specimen. Optical micrograph of the tempered specimens and control are shown in Figures 4.8-4.12.

ISSN: 2582-6271

Vol.1 No.2; 2020

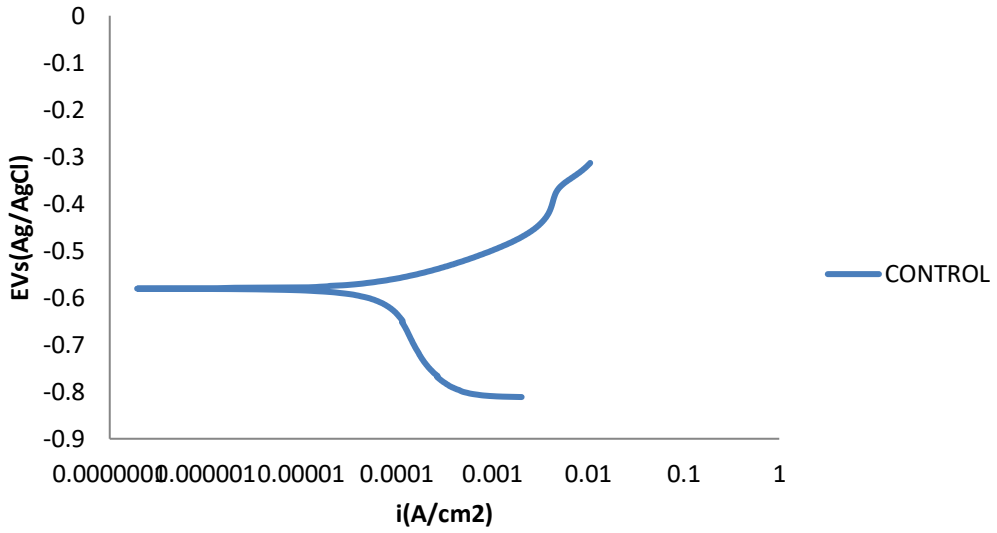

Figure 4.2. Tafel Plot of the control Specimen

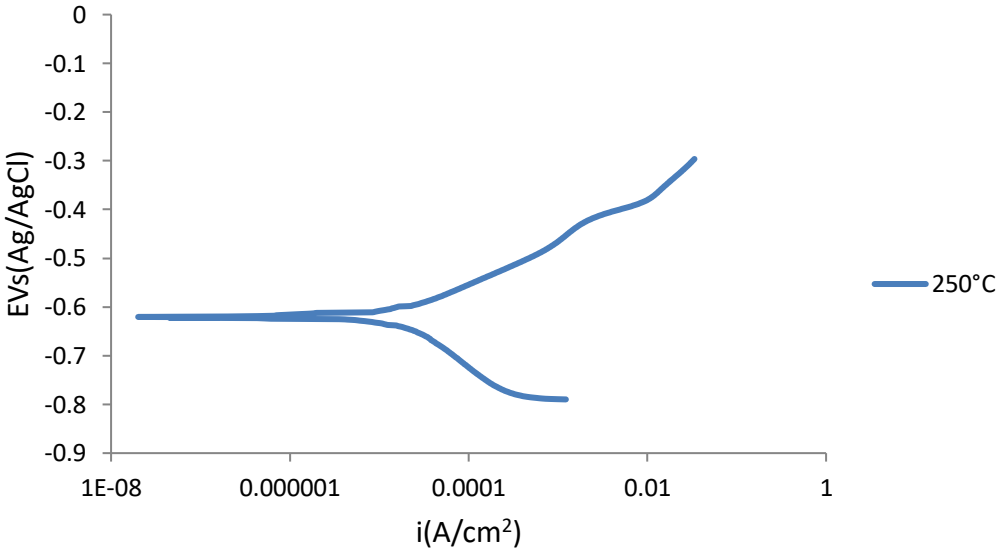

Figure 4.3. Tafel Plot of Tempered specimen at 250◦C

ISSN: 2582-6271

Vol.1 No.2; 2020

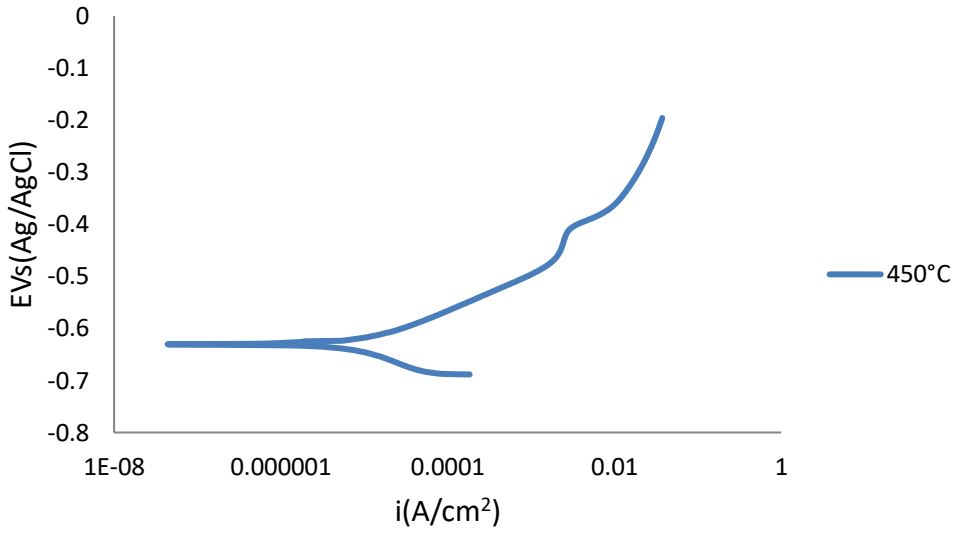

Figure 4.4. Tafel Plot of Tempered Specimen at 450◦C

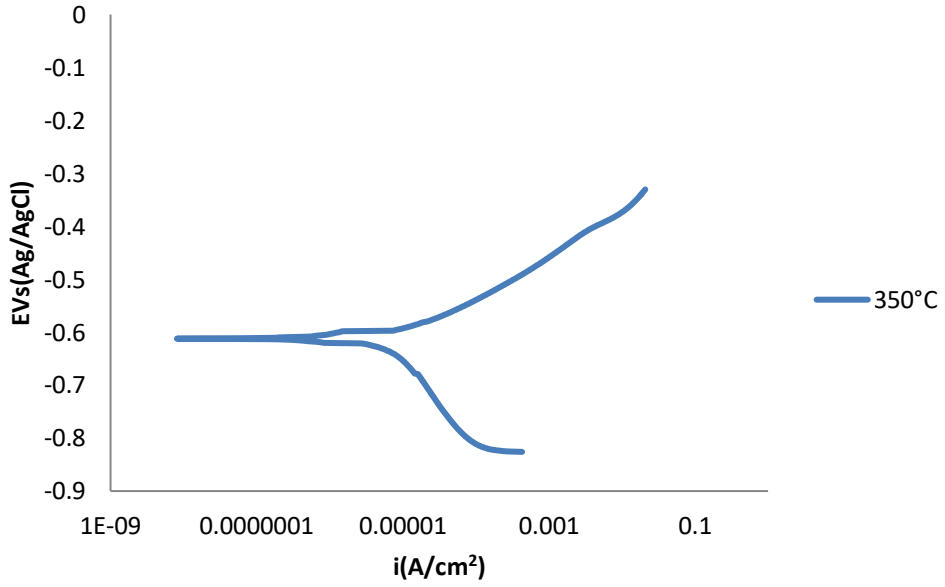

Figure 4.5. Tafel Plot of Tempered Specimen at 350°C

ISSN: 2582-6271

Vol.1 No.2; 2020

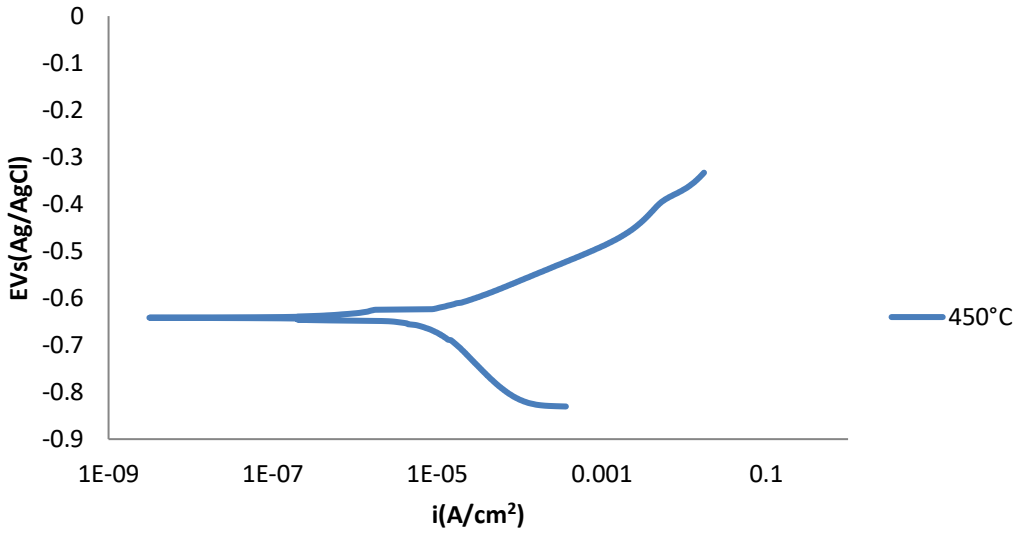

Figure 4.6. Tafel Plot of Tempered Specimen at 550°C

ISSN: 2582-6271

Vol.1 No.2; 2020

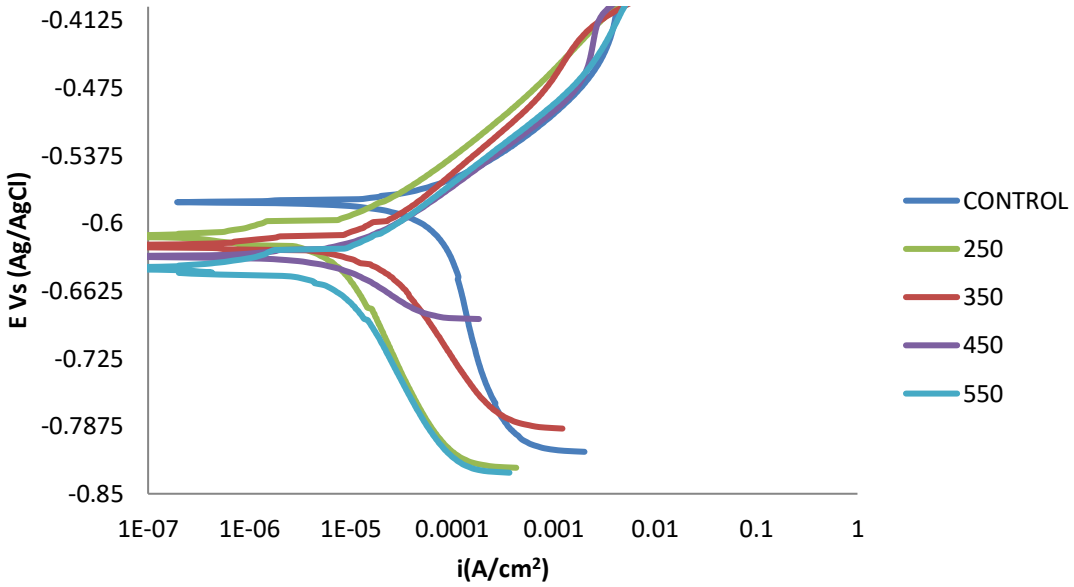

Figure 4.7. Graph Comparing Tafel Plots of the Specimens

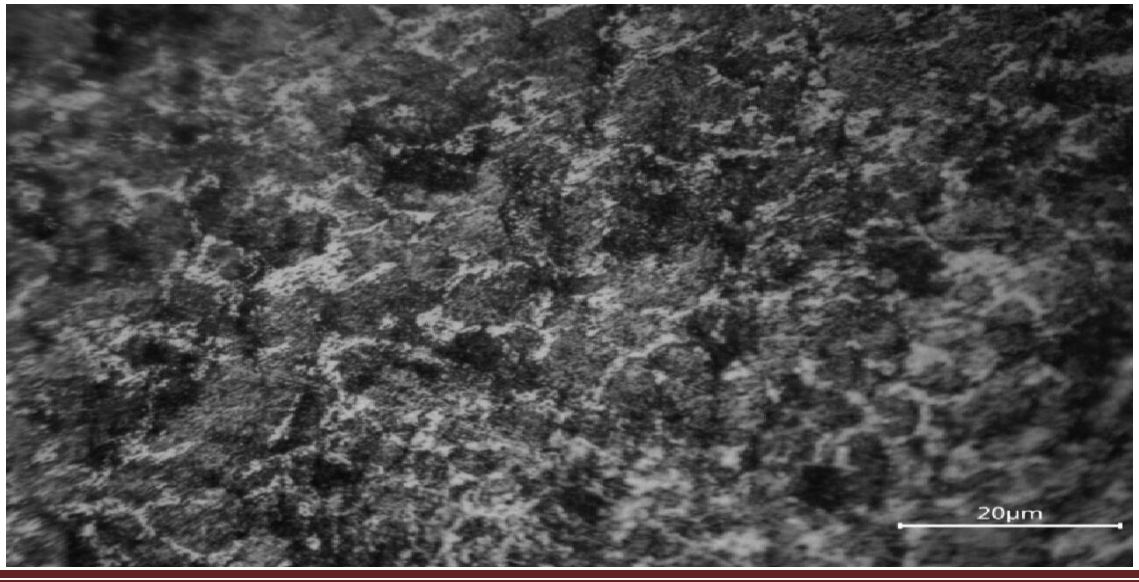

ISSN: 2582-6271

Vol.1 No.2; 2020

Figure 4.8. Optical Micrograph Image of Control Specimen Shown Under Magnification of X400
The microstructure consists dominantly of pearlite and finer ferrite grains, spread across the matrix.

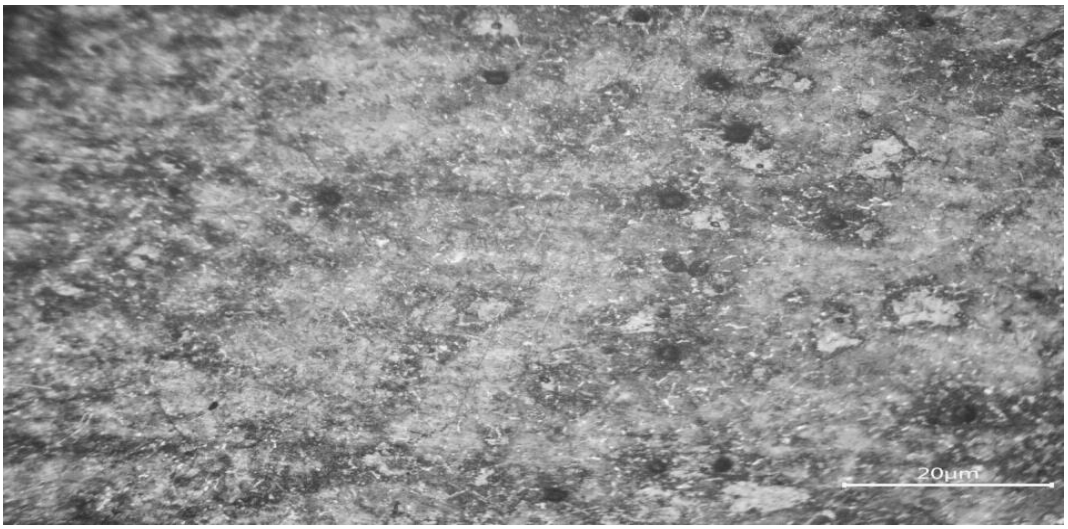

Figure 4.9. Optical Micrograph Image of 250oC Specimen Shown Under Magnification of X400

Shows presence of tempered martensite, cementite, retained austenite (light grey coloration) and ferrite precipitate in the microstructure.

ISSN: 2582-6271

Vol.1 No.2; 2020

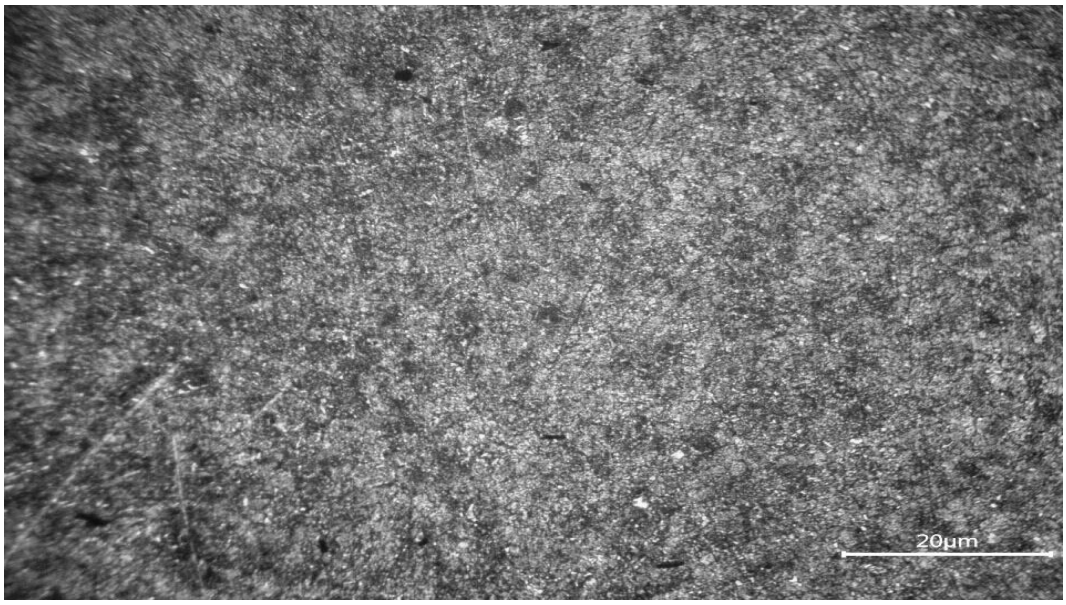

Figure 4.10. Optical Micrograph Image of 350oC Tempered Specimen Shown Under Magnification of X400

Shows a dark grey coloration signifying the present of martensite with sparsely disperse cementite particles amidst ferrite grains particles in the microstructure.

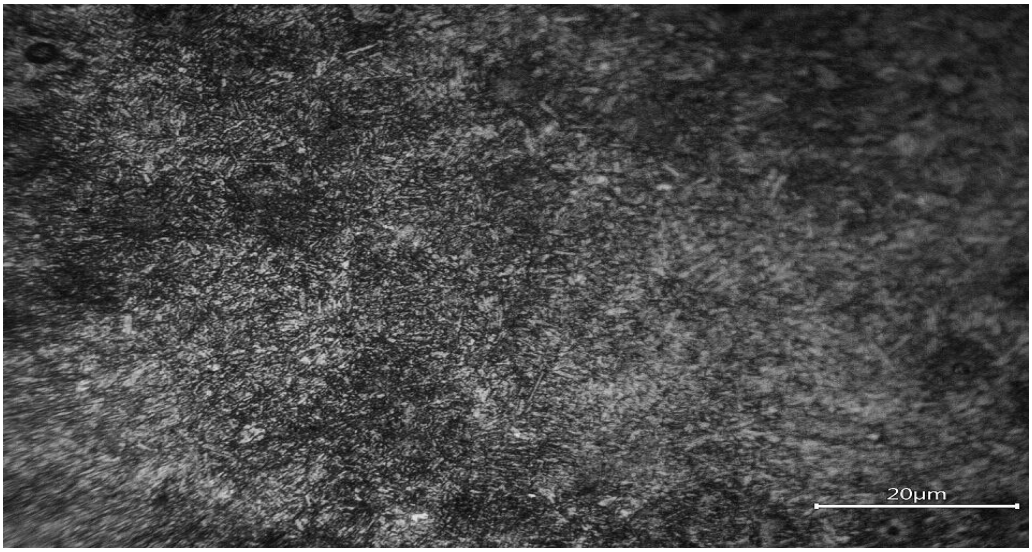

Figure 4.11. Optical Micrograph Image of 450oC Tempered Specimen Shown Under Magnification of X400

ISSN: 2582-6271

Vol.1 No.2; 2020

Shows a recrystallize ferrite grains and coarsened cementite particles, distribution uniformly in the matrix

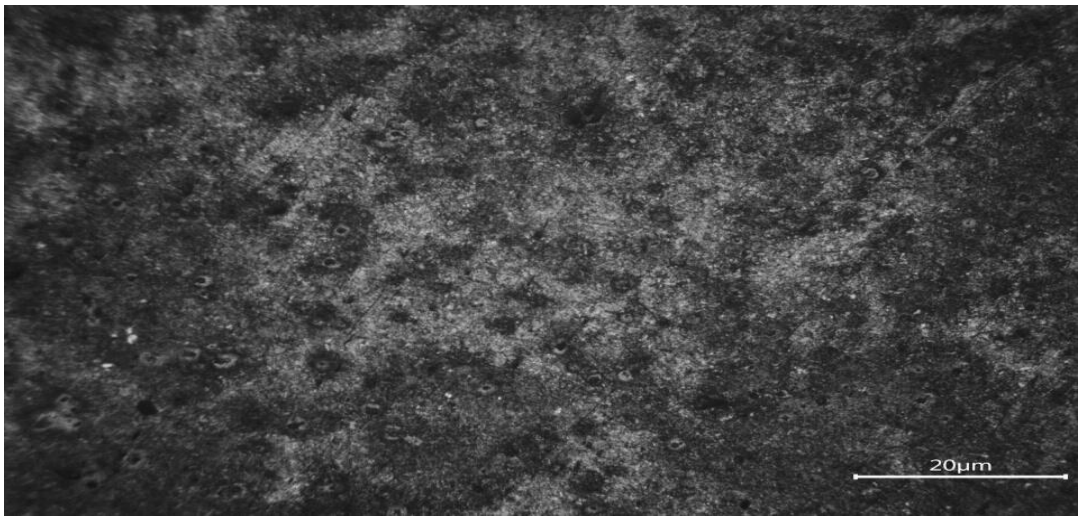

Figure 4.12. Optical Micrograph Image of 550oC Tempered Specimen Shown Under Magnification of X400

Micrograph Image reveals a highly recrystallized ferrite grains and more coarsened cementite particles within the matrix.

4.2 Discussion

4.2.1 Effect of Tempering on Microstructure

The micrograph in Figure 4.9-4.12 reveals microstructure of the quenched and tempered specimens. As shown in the images, the tempering temperatures generally altered the precipitate sizes, distributions and density of cementite in the iron matrix, as the specimens where tempered respectively at 2500C, 3500C, 4500C, 5500C for 30mins. The micrographs of the tempered specimens can best be explained in three transformation-stages; first stage is from 2500C- 3500C, second stage, 3500C-4500C and third stage, 4500C-5500C. In the first stage, meta-stable martensite decomposes into ferrite and unstable carbides, as shown in Figure 4.9, the light gray coloration signifies martensite phase while patches of dark marks depicts disperse particles of cementite which becomes more visible in the 3500C tempered specimen, as seen in Figure 4.10. In the second stage i.e. 3500C -4500C the meta-stable martensite might have been totally converted to more stable cementite precipitate as revealed in Figure 4.10, the uniformly dispersed

ISSN: 2582-6271

Vol.1 No.2; 2020

mottled dark spots depicts cementite grains amidst ferrite grains, which becomes more coarser within α-ferrite matrix as the tempering temperature was raised to 4500C, as seen in Figure 4.11. In the last stage; 4500C -5500C as shown in the micrograph image in Figure 4.12 the microstructure revealed more coarsened and stable cementite in the iron matrix. Micrograph image shows a sparsely dense, non-uniform distribution of cementite particles within the matrix and α-ferrite grains. This result is in accordance with the findings of Speich and Leslie [10], which stated the transformational stages of tempered carbon steels.

4.2.2 Effect of Tempering on the Corrosion Rate

The results of the corrosion rate of the tempered specimens and un-tempered specimen (control). Generally, the corrosion rates of the tempered specimens in sodium chloride medium (NaCl) is low when compared to the un-tempered specimen, as seen in Figure 4.1. For the tempered specimens, the corrosion current density (icorr) decreases with increasing tempering temperatures. It reveals the corrosion resistance of the tempered specimens has become better and better. Compared with the un-tempered specimen, the results for the corrosion current densities of the specimens after polarization was smaller, which demonstrate that the tempering temperatures have a certain corrosion resistance effect on the 0.42%C steel. Moreover, the corrosion rates of the four tempered specimens were calculated from the corrosion current densities taken from Tafel plot by Faraday's law, where C.R is the corrosion rate (mm/year), A is the area (in cm2), d is the density in (g/cm3), 0.13 is the metric and time conversion factor. Steel specimen tempered at 5500C has lower corrosion rate than steels tempered at 4500C, 3500C and 2500C, which demonstrates the corrosion resistance of 5500C tempered steel is higher than other steels. This is in agreement with the findings of Gebril et al. [11] where it was observed that lower tempered specimen showed higher corrosion rate and the corrosion rate decreases progressively in the higher tempered specimens. These changes in corrosion rate was attributed to the presence of finer second phase precipitate in tempered medium carbon steel which led to set up of galvanic cells which accelerated the corrosion rate while the decrease in the corrosion rate of the higher tempered above about 500°C, was as a result of the cementite coalesces into large particles.

4.2.3 Effect of Microstructural Change on the Corrosion Susceptibility

The corrosion rates of the specimens can be explained from the micrograph in Figure 4.8- 4.12. The microstructure in Figure 4.8 (Control specimen) showed the least corrosion resistance. The observable difference in corrosion rates could be attributed to microstructure formed as a result of the production process used (hot-rolled). The micrograph in Figure 4.9 revealed some presence of retained martensite (meta-stable), precipitate of cementite (dark) and α-ferrite. The combined effect of these tends to explain why 2500C gave higher corrosion compared with other tempered specimens. Subsequently Figure 4.10-4.12 showed increasing presence of cementite precipitate and α-ferrite. It was observed that the changes in the corrosion rate may be attributed to the ferrite precipitate and the density of carbide precipitated. The lower tempered micrograph showed densely dispersed cementite particles than the higher tempered

ISSN: 2582-6271

Vol.1 No.2; 2020

specimens that are sparsely distributed with coarse cementite particles, these led to reduced cathodic sites for electrochemical reaction. The result also tends to suggest that the more cementite coarsen (cathodic area), the more corrosion rate decreases. This is in agreement with the findings of Igwemezie and Ovri [12] where it was stated that corrosion rate in medium carbon steels changes with the rate of precipitation of ferrite and cementite phases.

5.1 CONCLUSIONS

From the investigation and comparison of the data obtained during the course of this work, the following conclusion were made on the effect of tempering temperature on the corrosion susceptibility of medium carbon steel in sodium chloride (NaCl) environment.

1. It was found that microstructural change has a marked effect on the corrosion rate, the importance of both the amount of cementite acting as cathode and ferrite acting as anode, this led to the setting up of micro-galvanic cell within the metal, the combined effect of micro-galvanic cell corrosion and its state of subdivision supports the electrochemical mechanism of corrosion.

2. The microstructure of medium carbon steels tempered at different temperatures directly affects the corrosion rate and as the distribution of cementite within the matrix decreases, the corrosion rate decrease.

3. Specimens tempered at higher temperatures gave lower corrosion rates in NaCl solution. This is attributed to the decomposition of meta-stable martensite and formation of coarse cementite grains at temperatures above 350°C, leaving the solid solution with coarse cementite grains adjoining the ferrite matrix.

4. The microstructure of tempered specimen at 3500C shows a uniform dispersion of coarse cementite and fairly good resistance to corrosion in NaCl environment than the lower tempered specimens, which revealed that, it is best to be used in this medium compared to other specimens.

REFERENCES

[1] Achebe CH. Nneke UC. Anisiji OE. Analysis of Oil Pipeline Failures in the Oil and Gas Industries in the Niger Delta Area of Nigeria. In: Proceedings of the International Multi Conference of Engineers and Computer Scientists 2012; 2:1274-1279.

[2] Ideozu MU. Safety and Risk Implications of Corrosion of Oil and Gas Facilities. Corrosion and Materials in the Oil and Gas Industries. Boca Raton CRC Press 2016: 674-677.

[3] Andrew P. Rogers CN Subsea pipeline engineering, 3rd ed. Penn wall, Oklahoma 2007.

[4] Onyekpe B. The Essentials of Metallurgy and Materials in Engineering. Benin city: Ambik Press. 2002.

ISSN: 2582-6271

Vol.1 No.2; 2020

[5] Ferhat M. Benchettara A. Amara SE. Najjar D. Corrosion behaviour of Fe-C alloys in a Sulfuric Medium. J. Mater. Environ. Sci, 2014; 5(4): 1059-1068.

[6] Ahmad Z. Principles of Corrosion Engineering and Corrosion Control. Oxford: Butterworth-Heinemann 2006; 91.

[7] Afolabi AS. Corrosion and Stress Corrosion Behaviours of Low and Medium Carbon Steels in Agro-Fluid Media. Leonardo Elec J of Pract and Tech 2007; 10: 55-66.

[8] Callister J. Material Science and Engineering: An Introduction. 6th ed. New York: John Wiley and Sons, Inc. 2006

[9] Burt V. Corrosion in the Petrochemical Industry, 2nd ed. Materials Park: ASM International 2015; 328

[10] Speich GR. Leslie WC. Tempering of steel. Metallurgical Trans 1972 3(5): 1043–1054.

[11] Gebril MA. Aldlemey MS. Abdessalam FK. Effect of Tempering on Mechanical Properties and Corrosion Rate of Medium and High Carbon Steel. Advanced Materials Research 2013; 685: 81-85.

[12] Igwemezie V. Ovri JEO. Investigation into the Effects of Microstructure on the Corrosion Susceptibility of Medium Carbon Steel. The International Journal of Engineering and Science 2013; 2(6): 11-26. 2013